Journal of Hazardous Materials 486 (2025) 136925

Contents lists available at ScienceDirect

Journal of Hazardous Materials

journal homepage: www.elsevier.com/locate/jhazmat

# Effective management of pre-existing biofilms using UV-LED through inactivation, disintegration and peeling

Liang Shen [a,*], Wenqi Chen [a], Jinyu He [a], Xueru Luo [a], Yang Mei [b], Baoping Zhang [b,c]

[a] Department of Chemical and Biochemical Engineering, College of Chemistry and Chemical Engineering, the Key Lab for Synthetic Biotechnology of Xiamen City, Xiamen University, Xiamen 361005, China
[b] Department of Electronic Engineering, Laboratory of Micro/Nano-Optoelectronics, Xiamen University, Xiamen, Fujian 361005, China
[c] Institute of Nanoscience and Applications (INA), Southern University of Science and Technology (SUSTech), Shenzhen 518055, China

## HIGHLIGHTS

- 275 nm UV-LED can inactivate biofilm-bound *E.coli* to 3.2 log at 346.5 mJ/cm$^2$, 660 μW/cm$^2$.
- Irradiance & irradiation time are conjugated in Bunsen-Roscoe law for disinfection.
- Oxidative degradation of EPS matrix explains biofilm disintegration caused by UV.
- 36.1 % PS & 32.1 % PN are degraded but not fully mineralized at 275 nm, 346.5 mJ/cm$^2$.
- Shear force peeling after UV irradiation is effective to remove biofilms in water.

## GRAPHICAL ABSTRACT

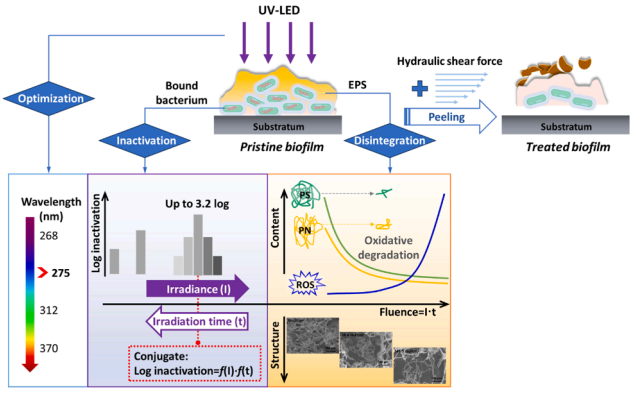


## ARTICLE INFO

*Keywords:*
UV-LED
Irradiation
Biofilm
EPS
Water disinfection

## ABSTRACT

Managing undesirable biofilms is a persistent challenge in water treatment and distribution systems. Although ultraviolet-light emitting diode (UV-LED) irradiation, an emerging disinfection method with the chemical-free and emission-adjustable merits, has been widely reported effective to inactivate planktonic bacteria, few studies have examined its effects on biofilms. This study aims to fill this gap by exploring the performance and mechanism of UV-LEDs on the prefabricated *Escherichia coli* (*E. coli*) biofilms under varying irradiation conditions. The results showed that the wavelength of 275 nm exhibited the best inactivation effect on the biofilm-bound *E.coli* compared to 268, 312 and 370 nm, achieving 3.2 log inactivation at a fluence of 346.5 mJ/cm$^2$ and an irradiance of 660 μW/cm$^2$. Furthermore, irradiance and irradiation time are proposed for the first time to be a pair of conjugate variables correlated to log inactivation, as a modification of the Bunsen-Roscoe reciprocity law. Additionally, the effect of UV irradiation on extracellular polymeric substances (EPS) in terms of the structure and chemical properties was investigated. The findings support that the oxidative degradation of the polysaccharides and proteins in EPS matrix should be the primary reason for destroying the biofilm framework. Finally, additional hydraulic shear was applied on the irradiated biofilms, suggesting an effective approach for enhancing biofilm removal.

* Corresponding author.
*E-mail address:* shenliang@xmu.edu.cn (L. Shen).

https://doi.org/10.1016/j.jhazmat.2024.136925
Received 8 October 2024; Received in revised form 3 December 2024; Accepted 15 December 2024
Available online 20 December 2024

## 1. Introduction

Bacteria thrive and proliferate in all kinds of aqueous environments, with more than 90 % existing in the form of biofilms. In artificial water and wastewater treatment systems, the interior walls of vessels and pipes provide ample placement for the formation and further development of biofilms. These unintended biofilms have many adverse consequences such as undermining the infrastructure hardware (biocorrosion), disturbing the operation process (biofouling), deteriorating the water quality (secondary contamination), and even causing sever public health risk (biofilm-associated infection). As well known, it is the extracellular polymeric substances (EPS) that bind bacteria and promote the adhesion of microbial cells to surfaces to form biofilms [1]. This protection from the EPS matrix, consisting of 75–90 % polysaccharides (PS) and proteins (PN) [2], could be lethal to humans if pathogens happen to be harbored within biofilms. So far in drinking water distribution systems, conventional disinfection using chlorine or chloramine continues to be the most frequently explored strategy for biofilm prevention and control. While, previous studies have shown that coliforms can persist in drinking water distribution system biofilms even in the presence of chlorine-based disinfectants [3]. If changing chlorine or chloramine to other new chemical agents, it confronts stringent requirements for approval under national policies and regulations [4]. In this context, physical ultraviolet (UV) irradiation has emerged as a promising alternative to conventional disinfectants for controlling biofilms in recent decades [5].

Considering the UV irradiation mechanism, wavelength and energy are commonly regarded two pivotal factors in the microbial disinfection systems. Absorption of UV photons by molecules leads to the absorbed energy released, triggering photochemical reactions that harm molecules. Although DNA and proteins have maximum absorbance around 260 and 280 nm, the optimal disinfection wavelength for UV spanning the range of 200–400 nm still needs exploration due to the complex composition of bio-macromolecules in biofilms. In this sense, ultraviolet-light emitting diode (UV-LED) has overwhelming superiority to mercury lamps for biofilms management. Because UV-LED can tailor wavelengths and irradiation modes through adjustable semiconductor configuration, generating wavelength in either UVC (200–280 nm), UVB (280–315 nm), or UVA (315–400 nm). Along with other merits, mercury-free UV-LEDs have emerged as the new generation of UV sources [6,7]. In 2010, Bak et al. [8] used a UV-LED (at 265 nm) to reduce the *Pseudomonas aeruginosa* biofilms inside urinary patient catheters, documenting the first application of UV-LED on pre-existing biofilms. Later, Gora et al. [9] expanded that research to the drinking water field by testing UV-LED (at 265 nm) against the *P. aeruginosa* biofilms grown on polycarbonate coupons. Additionally, Ma et al. [10] for the first time measured the UV absorption characteristics of the *P. aeruginosa* biofilms and further investigated the inactivation effect of UV-LEDs at 260 nm, 270 nm, and 282 nm on the biofilm-bound cells. However, the papers targeting the pre-existing biofilms are much less than those on planktonic bacteria [11-13], limiting the practical application of UV-LEDs to deal with the biofilm problem in water industry. We think that the difficulty lies in understanding the interaction between UV and EPS, a topic rarely addressed in literature. EPS can typically reduce the light penetration, which in turn increases the UV irradiation fluence and power energy to inactivate the biofilm-bound bacteria given the common dose-response relationship in chemical disinfection [14,15]. On the other side, destroying EPS beyond killing germs offers another way to manage biofilms by UV. It means that disintegration and peeling besides inactivation of interior bacteria may contribute the efficacy of UV irradiation on biofilms management. While, when EPS is considered as the third pivotal factor alongside wavelength and energy in the UV-LED and biofilm system, both the performance and mechanisms of this disinfection process become a more complex puzzle.

Therefore, to elucidate the disinfection effect and mechanism of UV-LED on biofilms, *Escherichia coli* (*E. coli*), an indicator bacterium for microbial water quality examination, was used to prepare model biofilms in this work. Then the static irradiation experiments were conducted with UV-LEDs emitting UV lights covering UVC, UVB and UVA. The specific questions include: (i) How do wavelength, fluence, irradiance and irradiation time affect inactivation efficiency? A new conjugation theory on energy was proposed to improve the conventional dose-inactivation equation. (ii) How does the UV irradiation change the structure and chemical composition of EPS in biofilms? The potential role of reactive oxygen species (ROS) induced by UV was also discussed. (iii) How does the UV irradiation alter biofilm adhesion strength? A potential strategy for biofilm removal using hydraulic shear force combined with UV irradiation was suggested.

## 2. Materials and methods

### 2.1. Bacterial culture and biofilm preparation

The wild type *E. coli* DH5α was incubated in 20 mL of Luria-Bertani (LB) medium at 37 °C, 200 rpm for 12 h to obtain the bacterial suspension. The method to prepare biofilms was referred to the static filter biofilm assay from Bjarnsholt et al. [16]. As shown in Fig. S1, two types of polyethersulfone (PES) filter membranes, with the same pore size of 0.22 μm but different diameters of 25 or 40 mm, were used as substratum for biofilm-bound bacteria disinfection and EPS irradiation experiments, respectively. Briefly, PES membranes were immersed in deionized water and sterilized, and then tiled on the top of the AB trace glucose (0.5 %) (ABTG) agar plate in an ultra-clean hood, preventing the generation of bubbles between the membrane and the plate. After drying for 10 min, 20 or 60 μL of the bacterial suspension was dripped on the PES membrane. Waiting for 5–10 min, the plate was sealed and incubated in a biochemical incubator at 37 °C for 24 h. The final biofilm samples appeared as circular plaques with diameter of ~9 or ~25 mm.

### 2.2. UV-LED irradiation experiment and inactivation quantification

Four UV-LEDs with specifications of 265, 275, 310 and 365 nm were purchased from Great Bright Company, China. Their normalized emission spectra were measured by Spectro 320 optical scanning spectrometer, exhibiting the peak wavelength of 268, 275, 312 and 370 nm, and the full width at half maximum (FWHM) of 15.6, 12.7,13.0 and 20.2 nm, respectively (Fig. S1). Two LED modules, equipped with 1 LED and 9 LEDs (3 × 3), were used for irradiation experiments on two kinds of biofilm samples with bacterial plaque diameter of 9 and 25 mm, respectively (Figs. S1b and c). The fluence is given by Eq. 1 [17].

$$F = I \cdot t \quad (1)$$

in which, F is the fluence representing the incident energy, mJ/cm$^2$, I is the irradiance representing the irradiation intensity, mW/cm$^2$, and t is the irradiation time, s.

For each irradiation experiment, the distance between the LED module and the biofilm sample was adjusted around 15–22 mm according to the pre-set irradiance, which was confirmed through the measurement at the same position on the sample surface using an IL-1700 radiometer with a SED 270 detector (USA International Light). Besides, the UV-LED was pre-lit for 5 min before irradiation to ensure stable light emission. All irradiation experiments were carried out in a dark room to reduce the photo repair of bacterial DNA damage.

The living bacterial in biofilms was enumerated by way of plate counting. After irradiation, the biofilm sample was transferred to normal saline, blown with a pipette gun and wiped with sterile cotton to resuspended the components in biofilms. The solution was then homogenized with a vortex meter for 3 min for further analysis. Briefly, the detachment from the irradiated and unirradiated (as control) biofilms was diluted in series (referring to a reasonable number of 50–300 col-

onies on each plate). Then, 100 μL of the diluent was smeared on the LB agar plate, cultured at 37 °C for 20 h, and the colony forming units (CFU) were counted. Log inactivation, the general decimal reduction factor to quantify the inactivation efficiency, is given by Eq. 2.

$$\text{Log inactivation} = \log\frac{N_0}{N_t} \quad (2)$$

in which, $N_0$ and $N_t$ are the microbial concentrations (CFU/mL) before UV irradiation and at UV irradiation time t.

### 2.3. Biofilm characterization

#### 2.3.1. Morphology and optical characteristics of pristine biofilm

Microscopic visualization on the pristine biofilm sample before irradiation was carried out using scanning electron microscopy (SEM, Hitachi S-4800, Japan) and atomic force microscopy (AFM, Asylum Research Cypher S, UK). The SEM sample was prepared following a gradient dehydration with ethanol and sprayed with platinum for 20 s, and then observed at a high pressure of 15 kT. The AFM image was processed using ultra-high frequency oscilloscope Analysis (version 3.00) software. The method for characterizing the UV absorbance of biofilm-bound bacteria and the transmittance of biofilms was modified from Ma et al. [10]. In short, the biofilm sample, as prepared in Section 2.1 and resuspended in Section 2.2, was scanned by a UV-*vis* spectrophotometer (UV-2550, Shimadzu, Japan) for UV absorption spectrum at 200–375 nm. Likewise, the opaque PES membrane was replaced by a quartz coupon as substratum to deposit biofilm samples. The UV of certain wavelength penetrating across the quartz coupon with and without biofilm was measured by UV visible spectrophotometer (Cary 50, Agilent, USA). Their discrepancy in percentage was remarked as the transmittance of biofilm. Each experiment was conducted in triplicate to minimize the error.

#### 2.3.2. Determination of ROS

In this experiment, the total quantity of intracellular and extracellular ROS induced by UV was measured by a commercial detection kit (Solarbio, China) using a fluorescent probe called 2,7-dichlorofluorescein diacetate (DCFH-DA). According to the protocol, 1 mL of 3 μM DCFH-DA (diluted with normal saline) was added to the biofilm samples in a confocal culture dish. After UV-LED irradiation, the biofilm samples were incubated in dark at 37 °C for 30 min, and then transferred to a 96-well plate. The fluorescence signal was determined by microplate reader (SpectraMas M3, Molecular Devices, UK) with the excitation and emission wavelengths of 488 and 525 nm, respectively. Each experiment was repeated more than 6 times.

### 2.4. EPS extraction and characterization

Similar to the inactivation experiment described in Section 2.2, the biofilm after UV irradiation was recovered and the swab was resuspended in ultrapure water for EPS extraction, according to the method in literature [18]. Namely, the sample solution was shaken at 45 ℃ (water bath) and 100 rpm for 1 h to promote the dissolution of EPS components, centrifuged at 10,000 g for 20 min, filtered with a 0.45 μm filter membrane and stored in a −20℃ refrigerator. After extraction, the amount of EPS was expressed as total organic carbon (TOC), measured by ROC analyzer (TOC-1 CPN, Shimadzu, Japan). The PS content was determined by phenol sulfuric acid method [19], with glucose as the standard. The PN content was determined by an improved BCA method [20], and bovine serum albumin (BSA) was used as the standard protein, detailed in Fig. S2.

The excitation-emission matrix (EEM) spectroscopy on EPS was conducted with a fluorescence spectrometer (F-7000, Hitachi, Japan), by changing the excitation wavelength from 200 to 550 nm in a 5 nm increment and scanning the emission spectrum from 200 to 550 nm in a 5 nm increment. The spectrum of ultrapure water was recorded as blank. The Fourier transform infrared spectroscopy (FTIR, Nicolet iS20, Thermo Fisher, USA) was also detected for the extracted EPS.

### 2.5. Biofilm peeling experiment

The PES membrane with the biofilm was sticked on the inner wall of a 15 mL centrifuge tube and completely immersed in the normal saline solution. Then the tube was hold in a shaker at 100 rpm for 8 min, generating water shear force and simulating the flow in pipe. The sloughed biomass in solution was analyzed by the UV-*vis* spectrophotometer for two parameters, i.e., optical density at 600 nm ($OD_{600\ nm}$) and absorbance at 254 nm ($Absorbance_{254\ nm}$), representing the quantity of bacterial cells and EPS released from the biofilm in the experiment, respectively. The peeling efficiency is thereafter defined as Eq. 3.

$$\text{Peeling efficiency}\ (\%) = \frac{Q}{Q'} \times 100 \quad (3)$$

in which, Q is the $OD_{600\ nm}$ or $Absorbance_{254\ nm}$ detected for the sloughed biomass in solution as described above. Q' is the referential value from the control biofilm that was totally transferred in solution as elaborated in Section 2.2.

## 3. Results and discussion

### 3.1. Blocking effect on UV by biofilm

The amount of *E. coli* biofilm bacteria cultured for 24 h was about $1.6 \times 10^8$ CFU/mL. Fig. 1**a** shows the original morphology of the biofilm before irradiation. It exhibits a color of light yellowish brown, owing to the production of various pigment substances such as humus. The SEM and AFM images indicate that the bacteria were densely packed together forming a rough chunky layer of 430.8 nm (Fig. 1b and 1c). EPS, as the protective film of bacterial cells, was amorphously entangled around the microorganisms, making it a cell cluster. The structure of the biofilm is like a sieve. Such a cross-linked network structure allows only part of the light to pass through [10,21,22]. Other micro-substance structures, mainly EPS components, shield light for embedded cells. The blocking effect of biofilm from UV irradiation was further validated through the UV absorption and transmittance measurement (Fig. 1d and 1e). The absorption spectrum of the pristine *E. coli* biofilms detached from the PES membrane was compared the latter with that of the *P. aeruginosa* biofilm fixed on the quartz coupon in reference [10]. As shown in Fig. 1d, the patten of two curves exhibits a high accordance, and the peak within 250–280 nm consists to the UV absorption ability of DNA and protein, reflecting a universal absorption feature of biofilms. The transmittance results of 60–80 % at 268, 275, 312 and 370 nm corresponding to four UV-LEDs are plotted in Fig. 1e, indicating that the experimental *E. coli* biofilm is translucent to UV light. Further analysis on Fig. 1d and 1e, it is seen that contrary to the absorbance, the transmittance increases along with the UV wavelength increment, which agrees with the previous finding that the penetration ability of UV photons in water system decreases with the decrease of wavelength [23]. That is to say, for biofilms, UVA has stronger penetration ability, whilst UVC has stronger bactericidal effect.

### 3.2. Disinfection performance of UV-LEDs with different wavelengths

Fig. 2a plots the fluence-inactivation response of *E. coli* biofilms exposed to different UV-LED wavelengths, using the same irradiance of 384 μW/cm$^2$ as that utilized for inactivating planktonic *E. coli* in our previous work [11]. All inactivation results in Fig. 2a present typical shoulder-tailing or sigmoidal curves. Among them, the wavelength of 275 nm showed higher log inactivation than the other three wavelengths of 268, 312 and 370 nm. This finding from biofilms accords well

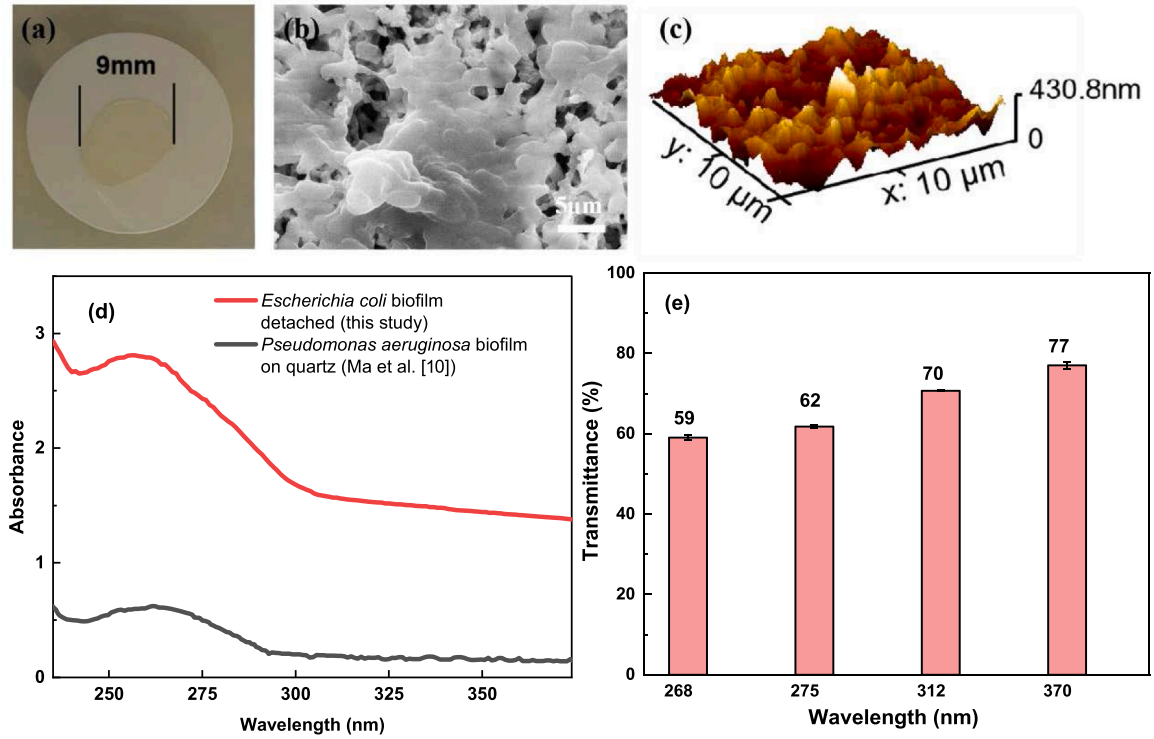


**Fig. 1.** The morphology of the pristine biofilm indicated by (a) optical camera; (b) SEM; (c) and AFM images. (d) Absorbance of the resuspension of the *E. coli* biofilm detached from the PES membrane, with referential spectrum of Ma et al. [10]. (e) UV transmittance of different wavelength across the *E. coli* biofilm on the quartz coupon.

with the observation from planktonic bacteria, indicating that UVC shows better bactericidal effect than UVB and UVA [7]. Generally, the three bands of UV execute different disinfection mechanisms for inactivating bacteria. UVA mainly causes the production of ROS in cells, destroys cell membrane and cell structure, and causes oxidative damage to cells. UVB irradiation mainly affects the endogenous substances of microorganisms to absorb photons and cause direct photoinactivation when the chemical structure changes. The main inactivation pathway for UVC disinfection is through pyrimidine dimerization [24]. Additionally reflected in Figs. 2a, 1.9-log inactivation for *E. coli* biofilms was achieved at the 275 nm and fluence of 115 mJ/cm$^2$. While, the results in the counterpart of planktonic *E. coli* [11] showed that 267 nm had better effect than 275 and 310 nm, and 1.9-log inactivation for planktonic *E. coli* was achieved at the 275 nm and fluence of ~8 mJ/cm$^2$, taking only ~7 % of that for biofilms. In other words, ~14-fold higher fluence is needed for biofilm to achieve equivalent log inactivation of planktonic bacteria. This discrepancy reflects the impact of EPS in the process of inactivating biofilm-bound bacteria, i.e., improving more weight of photochemical reactions on proteins than DNA and thereby consuming more UV energy. As well known, the peak absorption profile of microbe DNA depends on the exact composition of the adenine, guanine, thymine, and cytosine nucleotides. Similarly, biofilms have been found to have wavelength dependent responses to UV treatment known as the action spectrum [6]. Further, we changed the irradiance to 660 μW/cm$^2$ and repeated the experiments with the best two wavelengths of 268 and 275 nm to verify the effect of wavelength. The results in Fig. 2**b** confirm that in this study, the UV-LED with peak emission at 275 nm provides the best disinfection performance as 3.2-log inactivation for

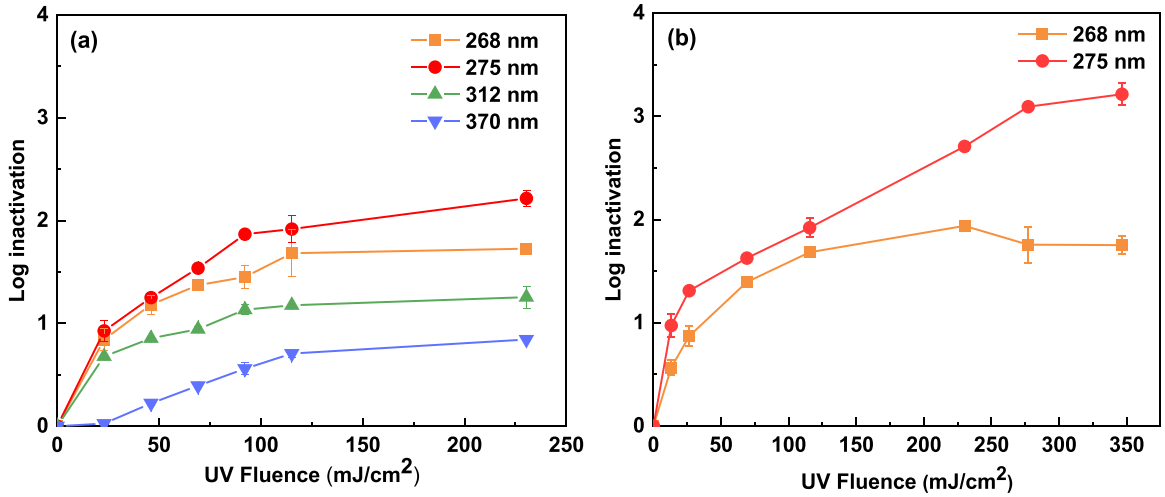


**Fig. 2.** Inactivation profile for *E. coli* biofilms exposed to: (a) 268, 275, 312, 370 nm UV-LEDs at 384 μW/cm$^2$; (b) 268, 275 nm UV-LEDs at 660 μW/cm$^2$.

biofilm-bound *E. coli* at 346.5 mJ/cm$^2$ and 660 μW/cm$^2$. This value of 3.2 is higher than the best performance of 2.1-log inactivation obtained from the 270 nm UV-LED on the biofilm-bound *P. aeruginosa* at 10 mJ/cm$^2$ [10], and has applicable meaning for water disinfect practice.

### 3.3. Irradiance and time: a pair of conjugate variables for UV disinfection effectiveness

As noticed in Fig. 2a and 2b (under 384 and 660 μW/cm$^2$, respectively), even keeping the same the wavelength and fluence, the UV disinfection results of *E. coli* biofilms were different. Thus, the variation of log inactivation along with irradiance under a certain fluence of 268 and 275 nm UV-LEDs was depicted in Fig. 3a and 3b, respectively. Interestingly in these figures, the height of columns in each cluster is not uniform, and there is a peak near the middle. This observation challenges the validity of the Bunsen-Roscoe law, implying that irradiance may separately affect log inactivation rather than simply acting as one of the two multipliers in fluence (seeing Eq. 1).

The classic Bunsen-Roscoe law, developed on photochemistry, is usually expressed as Eq. 4 for describing the photochemical effect on molecules or organisms [25,26].

$$E = f(F) \tag{4}$$

in which, E is the efficiency of the photochemical reaction, specifically refers to log inactivation for disinfection defined in Eq. 2; F is the fluence in Eq. 1; *f* represents the symbol of function. Combining Eq. 1 and Eq. 2, Eq. 4 can be rewritten as Eq. 5.

$$\text{Log inactivation} = f(I{\cdot}t) \tag{5}$$

According to Eq. 4 or Eq. 5, it can assert that for the same log inactivation it does not matter whether the fluence is reached with high irradiance and short irradiation time or with low irradiance and long irradiation time, that is why the Bunsen-Roscoe law also called the reciprocity law. Numerous studies have proven the validity of the Bunsen-Roscoe law to describe the UV inactivation behavior. However, apart from our finding in Fig. 3, there are many other reports not obeying the Bunsen-Roscoe law. Particularly for UV irradiation on *E. coli*, Rentschler et al. [27] for the first time questioned the Bunsen-Roscoe law using the low-pressure (LP) mercury lamp of 253.7 nm and *E. coli* seeded on Petri plates. And they found that "lower irradiance + longer time" resulted in higher log inactivation, for the same UV fluence. This statement was evidenced by the subsequent studies of Pousty et al. [28] and Matsumoto et al. [29] using UV-LEDs in range of 265–308 nm and *E. coli* in water. On the contrary, the argument of "higher irradiance + shorter time" was proposed by Sommer et al. [30]. They found that irradiance of 200 μW/cm$^2$ increased 1-log inactivation higher than that of 2 μW/cm$^2$, using LP mercury lamp and at equivalent UV fluences. Regarding the system of UV and biofilms, there is only one paper discussing the Bunsen-Roscoe law [9], in which the result is approximately in line with the latter hypothesis. For all these previous studies, no matter "lower irradiance + longer time" or "higher irradiance + shorter time", log inactivation was thought to follow a linear relationship with fluence, which could be explained through the deduction from the Chick-Watson disinfection law [31,32], a special form of the Bunsen-Roscoe law. Particularly, the Chick-Watson first--order linear model in case of UV irradiation is expressed as Eq. 6 [33].

$$\text{Log inactivation} = k{\cdot}F \tag{6}$$

in which, k is the inactivation constant.

Inserting Eq. 1 into Eq. 6 yields Eq. 7.

$$\text{Log inactivation} = k{\cdot}I{\cdot}t \tag{7}$$

Replacing the definition of log inactivation in Eq. 2, Eq. 7 transforms to Eq. 8 that is the fundament differential equation for the first-order kinetics.

$$\frac{dN_t}{dt} = K{\cdot}t, \quad K = -k{\cdot}I \tag{8}$$

in which, irradiance is part of the rate constant K; and irradiance should be independent with time.

Eq. 7 can explain the linearly variation of log inactivation with irradiance in literature, but not the non-linear change observed in Fig. 3, neither the disobedience to the Bunsen-Roscoe law. We think that the reason should lie in the relationship of irradiance and time. In our opinion, irradiance and time should be a pair of conjugate variables bearing a specific complementary relationship (analogy to a + bi and a - bi). Therefore, the correlation between disinfection performance and irradiance is expected to follow a reverse V-shape pattern, as exemplified by Fig. 3. The maximum log inactivation should be achieved when both irradiance and time are chosen at their respective medians. And the linear correlation reported in literature may be just located in the portion away from the peak. By such, we propose a new expression of the Bunsen-Roscoe law for UV disinfection as Eq. 9.

$$\text{Log inactivation} = f(I){\cdot}f(t) \tag{9}$$

### 3.4. Change of EPS in biofilms under different UV fluence

To investigate the effect of UV irradiation on the EPS matrix and its consequence for biofilm management, a series of characterization were

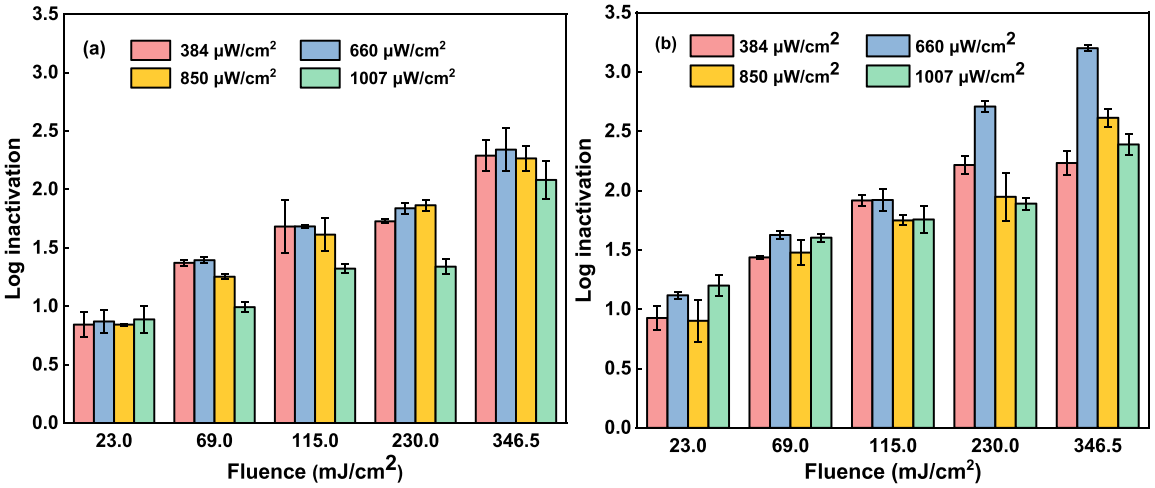


**Fig. 3.** Log inactivation of *E. coli* biofilms exposed to a certain UV fluence with variable irradiances, using (a) 268 nm and (b) 275 nm UV-LEDs.

implemented on the EPS extracted from *E. coli* biofilms under different UV fluence with the optimal wavelength of 275 nm and irradiance of 660 μW/cm$^2$, as exhibited in Figs. 4–8. The fluence value at zero indicated the control from the pristine biofilm without UV irradiation.

The SEM images in Fig. 4 showed that the integrity of EPS changed significantly, from a dense hydrogel structure to loosen macro-porous structure along with the increase of UV fluence, which is intuitive evidence for the disintegrating effect on biofilms caused by UV irradiation. Further, Fig. 5 presents the changes on the EPS quantity along with the UV fluence increasing from 0 mJ/cm$^2$ to 346.5 mJ/cm$^2$, in which TOC (reflecting the total amount of EPS) is almost kept unchanged but up to 36.1 % and 32.1 % of PS and PN reduced. It complies with the previous results from the planktonic bacteria that UV irradiation can decompose the high molecular weight components (e.g., PS and PN) of EPS [34,35]. And the discrepancy between left and right columns (representing TOC and PS+PN, respectively) suggests that during UV irradiation, PS and PN should be oxidized to soluble low molecular weight substances, rather than being completely mineralized to $CO_2$. Besides, the discrepancy on the UV induced decrement between PS and PN appears contrary to the general belief "more decomposition of PN than PS by UV" [1]. These findings inspire us to further consider the reactivity of EPS and the probable photo-generated ROS.

Figs. 6 and 7 are spectra of EEM and FTIR, respectively, for the same EPS samples under different fluence. In Fig. 6, regions I and II represent aromatic proteins; regions III and V are humus substances; and region IV is mainly some soluble microbial by-products [36]. Compared to the control, the fluorescence intensity of all regions decreased after UV irradiation, in a negative correlation to fluence. The most noticeable decrease of microbial by-products as shown in the region IV could be attributed to the weakened microbial activity of bacteria subjected to UV stress. The signal fading off in regions I and II confirms the PN decomposition observed in Fig. 5, and accords with the observation in EEM spectra from irradiating *Synechocystis* sp. at 312 nm [35]. And the decrease of fluorescence intensity in the region V also indicates that UV irradiation can degrade some humic substances [37]. In the FTIR spectra of Fig. 7, four peaks characterizing PS and PN gradually become sharp when fluence rising from 0 to 346.5 mJ/cm$^2$, i.e., the -OH of carboxylic acids, sugars and other substances at 3416 cm$^{-1}$, the C═O stretching vibration in the secondary structure of protein at 1647 cm$^{-1}$, the

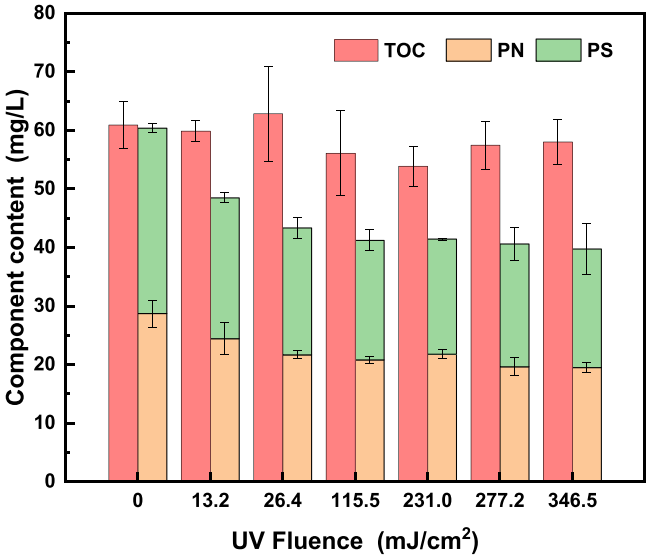


**Fig. 5.** Content of the EPS extracted from *E. coli* biofilms under different UV fluence (wavelength: 275 nm; irradiance: 660 μW/cm$^2$).

multiple C-OH symmetric stretching vibrations in the carboxyl group and polysaccharide during the deprotonation of aspartic acid at 1400 cm$^{-1}$ and 1099 cm$^{-1}$, respectively. This result demonstrates that PS and PN in EPS were effectively oxidized to carboxyl groups, which is similar to the conclusion derived from the planktonic *P. putida* MX-2 after irradiation by 254 nm LP mercury lamp [34].

Finally, Fig. 8 showed that the ROS generated in biofilms largely increased with UV fluence, which confirms the contribution of ROS oxidation in the aforementioned photodegradation of EPS. Besides, the effect of ROS against *E. coli* in biofilms has also been verified in literature [38]. Remarkably, it was observed in Fig. 5 that the degradation of PS and PN gradually slowed down when UV fluence exceeding 115.5 mJ/cm$^2$. But in Fig. 8, ROS initiated the exponential growth of at 115.5 mJ/cm$^2$. This can be ascribed to the more competitive ROS-ROS "self--destruction" reaction, rather than the oxidation of EPS and cells,

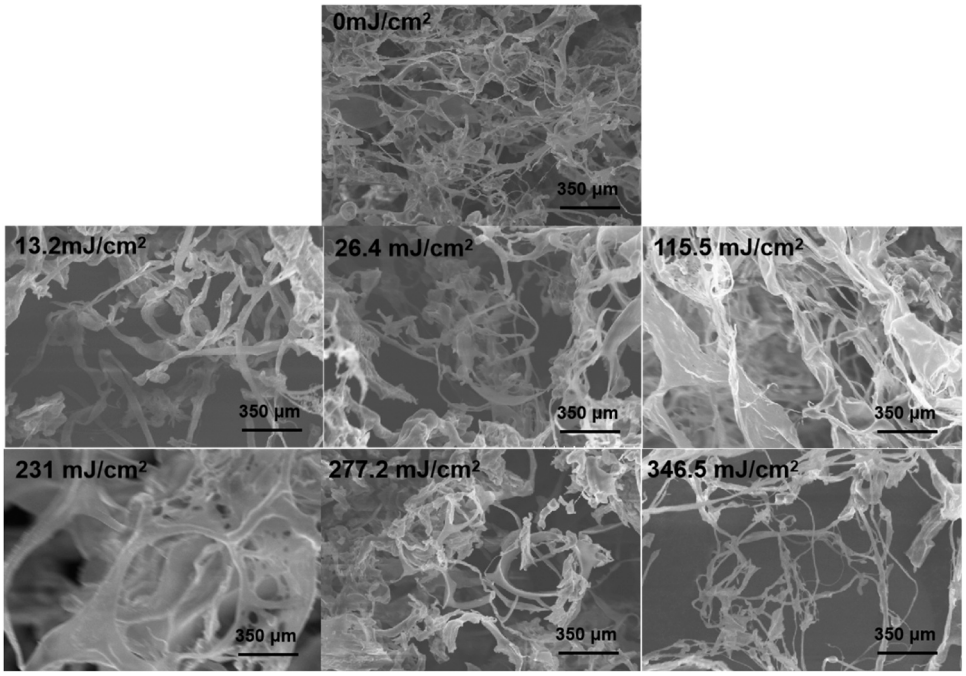


**Fig. 4.** The SEM images of the EPS extracted from *E. coli* biofilms under different UV fluence (wavelength: 275 nm; irradiance: 660 μW/cm$^2$).

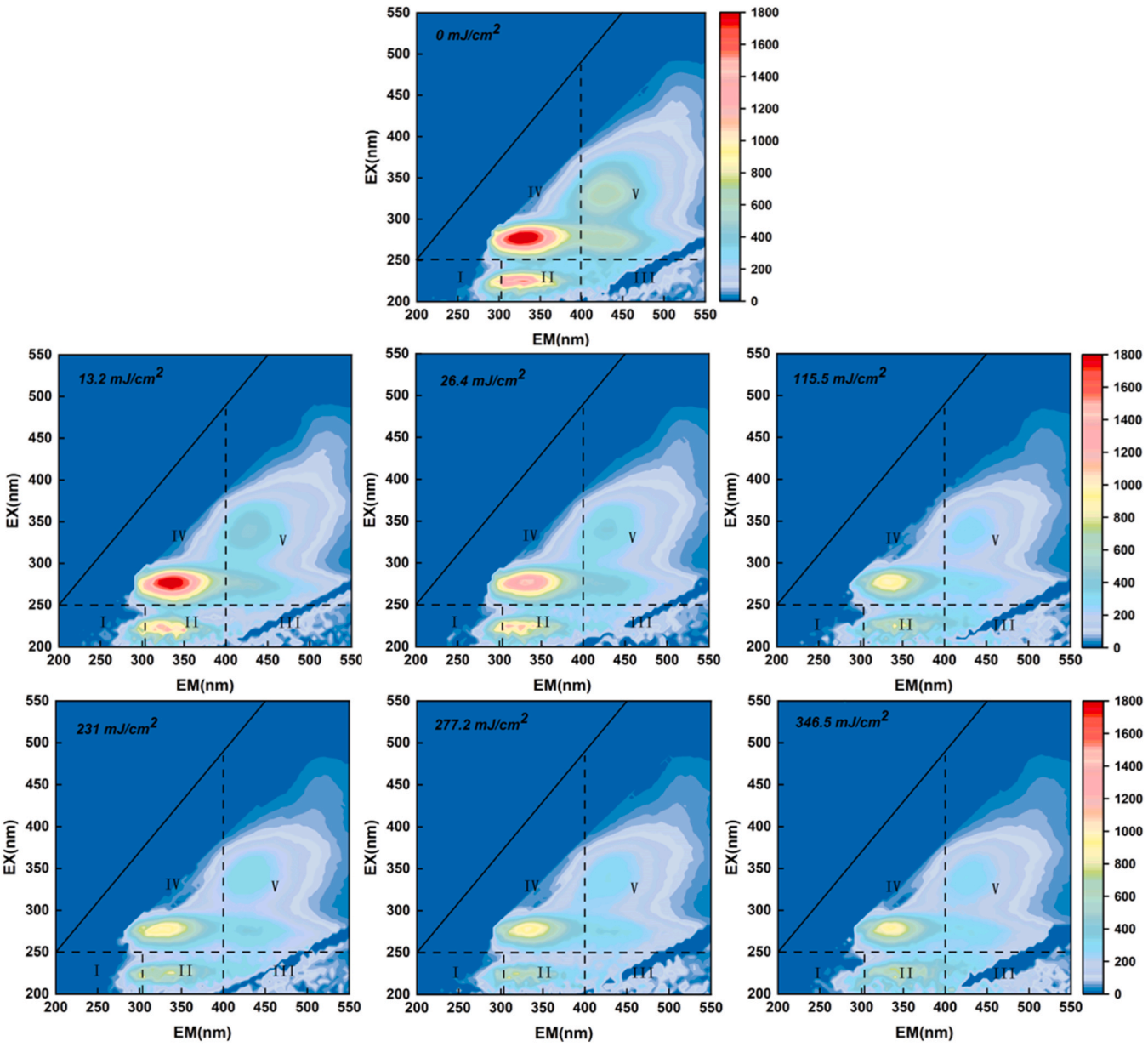


**Fig. 6.** The fluorescence excitation-emission matrix spectra of the EPS extracted from *E. coli* biofilms under different UV fluence (wavelength: 275 nm; irradiance: 660 μW/cm$^2$).

happened at high concentration of ROS [28]. Addition, some enzymes present in the EPS matrix, such as catalase and superoxide dismutase, may act as ROS scavenger [39-41].

### 3.5. Effects of UV irradiation on biofilm adhesion strength

After irradiated by 275 nm UV-LED, the adhesion strength of biofilms under water shear force was evaluated by peeling efficiency (Fig. 9). Apparently, no matter calculated from $OD_{600}$ or $Absorbance_{254}$ (representing the detached EPS), the peeling efficiency of the UV irradiated biofilms was greater than that of the control biofilm. Besides, when the UV fluence rising from 0 to ~346.5 mJ/cm$^2$, the peeling efficiency of the biofilm gradually increased from ~20 % to ~40 %, approaching to the equilibrium as the limitation of this pre-treatment technique. It indicates that UV irradiation can weaken the adhesion strength and increase the probability of biofilm slough from substratum. Previous studies have shown that UVC irradiation can greatly reduce the adhesion of planktonic bacteria to form biofilm [42]. And the detachment of biofilms has been speculated to bacterial death and EPS depolymerization [5]. In this study, the results regarding the inactivation of biofilm-bound bacterial and the change of EPS agree well with the effect of UV irradiation on destroying the adhesion of bacteria to the substratum (including other bacterial cells). The post-treatment of UV irradiation using a simple hydraulic shear is thereby suggested an effective way for removing the pre-existing biofilms. While, considering the cost of energy consumption, it seems that a reasonable peeling efficiency should be achieved in the hind side of the testing fluence of 0–346.5 mJ/cm$^2$ (locating at ~250 mJ/cm$^2$ in Fig. 9). The operational conditions for this biofilm peeling technique still needs to be optimized case by case in future.

### 3.6. Extensive discussion by integrating the subsection results

To manage the undesirable biofilms, four UV-LEDs emitting 268, 275, 312 and 370 nm were trialed on the prefabricated biofilm layer with thickness of 430.8 nm, composed by live *E. coli*. The transmittance

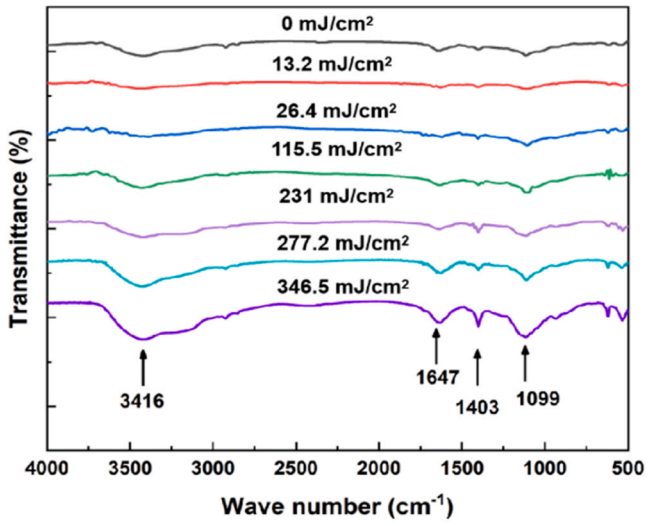


**Fig. 7.** The FITR spectra of the EPS extracted from *E. coli* biofilms under different UV fluence (wavelength: 275 nm; irradiance: 660 μW/cm$^2$).

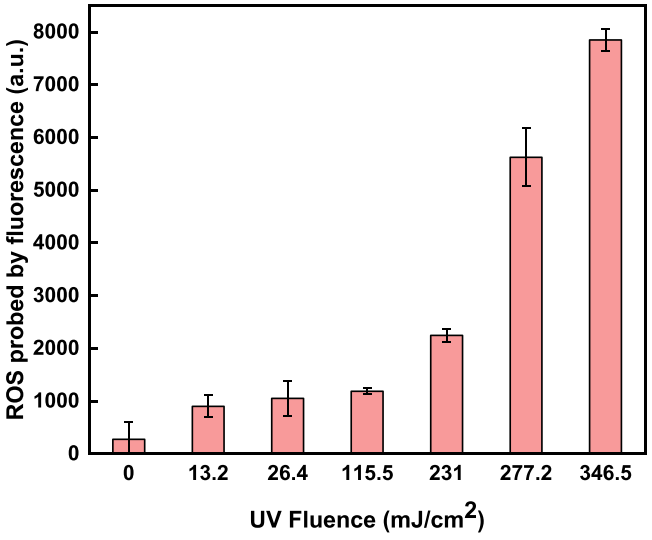


**Fig. 8.** The ROS induced by UV irradiation under different UV fluence (wavelength: 275 nm; irradiance: 660 μW/cm$^2$).

results of 60–80 % confirms the shielding effect of biofilms, in a reverse correlation with wavelength of UV. UVC, though weak at penetration, remains advantages in absorbance and germicidal ability. Further by comparing the log inactivation from different irradiation experiments, the disinfection effect of four wavelengths was ranked as: 275 nm > 265 nm > 312 nm > 370 nm. Among all tested biofilms in this study, the highest log inactivation of 3.2 was achieved by 275 nm UV-LED at a fluence of 346.5 mJ/cm$^2$ and an irradiation of 660 μW/cm$^2$. And ~14-fold higher fluence is found for biofilm to achieve equivalent log inactivation of planktonic bacteria. It suggests that UV-LED should be workable for sterilizing biofilm, but the question about increasing log inactivation by cost of high energy should be reconsidered. Hence, we investigated the reciprocal phenomena of two multipliers in the fluence determination formula, i.e., irradiance and irradiation time, by maintaining fluence and varying irradiance in irradiation experiments. Then for the first time, we propose a hypothesis that irradiance and time should be a pair of conjugate variables correlated to log inactivation, as expressed in Eq. 9 as a new expression of the Bunsen-Roscoe law for UV disinfection. According to this hypothesis, the log inactivation could be optimized by searching an ideal combination of irradiance and time,

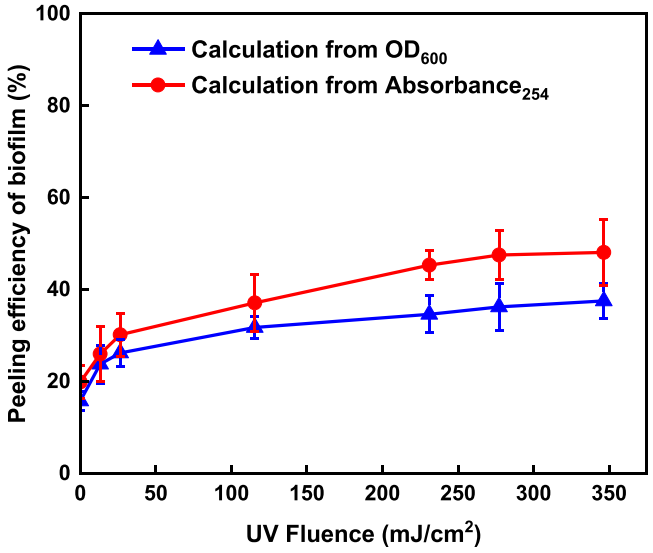


**Fig. 9.** The peeling efficiency of biofilms after 275 nm UV-LED irradiation with different UV fluence. The water shear force derived from shaking at 100 rpm.

even under a constant fluence.

While, considering the role of EPS, destroying biofilm integrity apart from inactivating biofilm-bound bacteria was proposed for biofilm management, which is validated by experiments as well. Comparing the EPS samples extracted from biofilms subject to UV irradiation at 275 nm from 0 to 346.5 mJ/cm$^2$, the structure became more porous and looser. The content of PS and PN decreased 36.1 % and 32.1 %, respectively. Meanwhile the total amount of EPS indicated by TOC was unchanged. Further evidenced by the spectra of EEM and FTIR, it demonstrates that PS and PN should be oxidized to soluble low molecular weight substances, rather than being completely mineralized to $CO_2$. The UV induced ROS was also detected in biofilms in an exponential relationship with fluence. Whereas, the amount of the ROS was not in line with the decay of PS and PN, implying a complicate photodegradation mechanism underlying the biofilm disintegration. Finally, inspired by the decomposition results of EPS, a simple shaking experiment was conducted to validate the weakening adhesion effect of UV irradiation on biofilms. Specifically, the hydraulic shear coming from 100 rpm caused an improvement around 2-fold higher removal for the irradiated biofilms than the counterpart. All these results shed light on the UV-LED irradiation as an effective technique for treating inevitable biofilms in the infrastructure of water industry, by way of inactivation, disintegration and peeling.

## Environmental implication

Unwanted but ubiquitous biofilms in water and wastewater systems are highly hazardous events, leading to problems like microbial contamination, biocorrosion and particularly pathogens habitation. Ultraviolet (UV) irradiation is a non-chemical alternative of the conventional disinfection technique chlorination. While so far, most UV disinfection studies focused on planktonic bacteria but not biofilms. Besides, the conventional UV light source mercury lamp has evolved to UV-light emitting diode (UV-LED). This study will bridge the gap of the new technology (UV-LED irradiation) and the old problem (biofilm control), and then provide new insights and useful reference for effective management of biofilms in water infrastructure.

## 5. Conclusions

The following conclusions can be drawn:

(1) UV-LEDs can inactivate the biofilm-bound bacteria, degrade the

EPS matrix, and reduce the biofilm adhesion strength. It suggests that UV-LEDs have the potential to serve as a destruction strategy for the pre-existing biofilms in water treatment and distribution systems.

(2) Regarding the inactivation of the biofilm-bound *E.coli*, 275 nm UV-LED achieved the best performance of up to 3.2 log inactivation at a fluence of 346.5 mJ/cm$^2$ and an irradiance of 660 μW/cm$^2$, among four UV-LEDs with wavelengths of 268, 275, 312 and 370 nm. And for the first time, it is proposed that irradiance and irradiation time in the Bunsen-Roscoe reciprocity law should be a pair of conjugate variables correlated to log inactivation.

(3) Regarding the destruction of the EPS matrix, although EPS cannot be fully mineralized by UV irradiation, as much as 36.1 % PS and 32.1 % PN can be degraded at 275 nm and 346.5 mJ/cm$^2$. Oxidative degradation is believed to be the primary cause of biofilm disintegration upon UV exposure.

(4) Regarding the reduction of the biofilm adhesion strength, the interior structure of the biofilm becomes loosened after UV irradiation. Therefore, the pre-treatment by UV-LEDs can mitigate the difficulty of mechanically peeling off unwanted biofilms in water using shear force.

## CRediT authorship contribution statement

**Liang Shen:** Writing – original draft, Supervision, Funding acquisition, Conceptualization. **Wenqi Chen:** Investigation, Formal analysis, Data curation. **Jinyu He:** Validation, Software, Methodology. **Xueru Luo:** Methodology, Data curation. **Yang Mei:** Resources, Methodology. **Baoping Zhang:** Writing – review & editing, Project administration.

## Declaration of Competing Interest

The authors declare the following financial interests/personal relationships which may be considered as potential competing interests: Liang Shen reports financial support was provided by National Natural Science Foundation of China. Liang Shen reports was provided by Natural Science Foundation of Fujian Province of China. If there are other authors, they declare that they have no known competing financial interests or personal relationships that could have appeared to influence the work reported in this paper.

## Acknowledgements

This work was supported by the National Natural Science Foundation of China (No. 22178293, 62234011, U21A20493), the Natural Science Foundation of Fujian Province of China (No. 2022J01022).

## Appendix A. Supporting information

Supplementary data associated with this article can be found in the online version at doi:10.1016/j.jhazmat.2024.136925.

## Data Availability

Data will be made available on request.

## References

[1] Chen, G.Q., Wu, Y.H., Wang, Y.H., Chen, Z., Tong, X., Bai, Y., Luo, L.W., Xu, C., Hu, H.Y., 2021. Effects of microbial inactivation approaches on quantity and properties of extracellular polymeric substances in the process of wastewater treatment and reclamation: a review. J Hazard Mater 413, 125283.
[2] Tsuneda, S., Aikawa, H., Hayashi, H., Yuasa, A., Hirata, A., 2003. Extracellular polymeric substances responsible for bacterial adhesion onto solid surface. FEMS Microbiol Lett 223 (2), 287–292.
[3] Murphy, H.M., Payne, S.J., Gagnon, G.A., 2008. Sequential UV- and chlorine-based disinfection to mitigate *Escherichia coli* in drinking water biofilms. Water Res 42 (8), 2083–2092.
[4] Oliveira, I.M., Gomes, I.B., Simões, L.C., Simões, M., 2024. A review of research advances on disinfection strategies for biofilm control in drinking water distribution systems. Water Res 253, 121273.
[5] Luo, X., Zhang, B., Lu, Y., Mei, Y., Shen, L., 2022. Advances in application of ultraviolet irradiation for biofilm control in water and wastewater infrastructure. J Hazard Mater 421, 126682.
[6] Rauch, K.D., MacIsaac, S.A., Reid, B., Mullin, T.J., Atkinson, A.J., Pimentel, A.L., Stoddart, A.K., Linden, K.G., Gagnon, G.A., 2024. A critical review of ultra-violet light emitting diodes as a one water disinfection technology. Water Res X 25, 100271.
[7] Song, K., Mohseni, M., Taghipour, F., 2016. Application of ultraviolet light-emitting diodes (UV-LEDs) for water disinfection: a review. Water Res 94, 341–349.
[8] Bak, J., Ladefoged, S.D., Tvede, M., Begovic, T., Gregersen, A., 2010. Disinfection of *Pseudomonas aeruginosa* biofilm contaminated tube lumens with ultraviolet C light emitting diodes. Biofouling 26 (1), 31–38.
[9] Gora, S.L., Rauch, K.D., Ontiveros, C.C., Stoddart, A.K., Gagnon, G.A., 2019. Inactivation of biofilm-bound *Pseudomonas aeruginosa* bacteria using UVC light emitting diodes (UVC LEDs). Water Res 151, 193–202.
[10] Ma, B., Seyedi, S., Wells, E., McCarthy, D., Crosbie, N., Linden, K.G., 2022. Inactivation of biofilm-bound bacterial cells using irradiation across UVC wavelengths. Water Res 217, 118379.
[11] Nyangaresi, P.O., Qin, Y., Chen, G., Zhang, B., Lu, Y., Shen, L., 2018. Effects of single and combined UV-LEDs on inactivation and subsequent reactivation of *E. coli* in water disinfection. Water Res 147, 331–341.
[12] Nyangaresi, P.O., Qin, Y., Chen, G., Zhang, B., Lu, Y., Shen, L., 2019. Comparison of the performance of pulsed and continuous UVC-LED irradiation in the inactivation of bacteria. Water Res 157, 218–227.
[13] Shen, L., Griffith, T.M., Nyangaresi, P.O., Qin, Y., Pang, X., Chen, G., Li, M., Lu, Y., Zhang, B., 2020. Efficacy of UVC-LED in water disinfection on *Bacillus* species with consideration of antibiotic resistance issue. J Hazard Mater 386, 121968.
[14] Bak, J., Ladefoged, S.D., Tvede, M., Begovic, T., Gregersen, A., 2009. Dose requirements for UVC disinfection of catheter biofilms. Biofouling 25 (4), 289–296.
[15] Maganha de Almeida, A.C., Quilty, B., 2016. The response of aggregated *Pseudomonas putida* CP1 cells to UV-C and UV-A/B disinfection. World J Microbiol Biotechnol 32 (11), 185.
[16] Bjarnsholt, T., Alhede, M., Jensen, P.Ø., Nielsen, A.K., Johansen, H.K., Homøe, P., Høiby, N., Givskov, M., Kirketerp-Møller, K., 2014. Antibiofilm properties of acetic acid. Adv Wound Care 4 (7), 363–372.
[17] Bolton, J.R., Linden, K.G., 2003. Standardization of methods for fluence (UV dose) determination in bench-scale UV experiments. J Environ Eng 129 (3), 209–215.
[18] Wu, Y., Chen, Z., Li, X., Wang, Y., Liu, B., Chen, G., Luo, L., Wang, H., Tong, X., Bai, Y., Xu, Y., Ikuno, N., Li, C., Zhang, H., Hu, H., 2021. Effect of ultraviolet disinfection on the fouling of reverse osmosis membranes for municipal wastewater reclamation. Water Res 195, 116995.
[19] Albalasmeh, A.A., Berhe, A.A., Ghezzehei, T.A., 2013. A new method for rapid determination of carbohydrate and total carbon concentrations using UV spectrophotometry. Carbohydr Polym 97 (2), 253–261.
[20] Lim, K., Parameswaran, P., 2022. Critical evaluation of heat extraction temperature on soluble microbial products (SMP) and extracellular polymeric substances (EPS) quantification in wastewater processes. Water Sci Technol 85 (8), 2318–2331.
[21] Quan, K., Hou, J., Zhang, Z., Ren, Y., Peterson, B.W., Flemming, H.C., Mayer, C., Busscher, H.J., van der Mei, H.C., 2022. Water in bacterial biofilms: pores and channels, storage and transport functions. Crit Rev Microbiol 48 (3), 283–302.
[22] Zhang, T.C., Bishop, P.L., 1994. Density, porosity, and pore structure of biofilms. Water Res 28 (11), 2267–2277.
[23] Chevremont, A.C., Farnet, A.M., Coulomb, B., Boudenne, J.L., 2012. Effect of coupled UV-A and UV-C LEDs on both microbiological and chemical pollution of urban wastewaters. Sci Total Environ 426, 304–310.
[24] Martín-Sómer, M., Pablos, C., Adán, C., van Grieken, R., Marugán, J., 2023. A review on LED technology in water photodisinfection. Sci Total Environ 885, 163963.
[25] Bunsen, R., Roscoe, H., 1863. Photochemische Untersuchungen. Ann Phys 193 (12), 529–562.
[26] Lang, H., Riesenberg, D., Zimmer, C., Bergter, F., 1986. Fluence-rate dependence of monophotonic reactions of nucleic acids in vitro and in vivo. Photochem Photobiol 44 (5), 565–570.
[27] Rentschler, H.C., Nagy, R., Mouromseff, G., 1941. Bactericidal effect of ultraviolet radiation. J Bacteriol 41 (6), 745–774.
[28] Pousty, D., Hofmann, R., Gerchman, Y., Mamane, H., 2021. Wavelength-dependent time–dose reciprocity and stress mechanism for UV-LED disinfection of *Escherichia coli*. J Photochem Photobiol B: Biol 217, 112129.
[29] Matsumoto, T., Tatsuno, I., Yoshida, Y., Tomita, M., Hasegawa, T., 2022. Time-dose reciprocity mechanism for the inactivation of *Escherichia coli* explained by a stochastic process with two inactivation effects. Sci Rep 12 (1), 22588.
[30] Sommer, R., Haider, T., Cabaj, A., Pribil, W., Lhotsky, M., 1998. Time dose reciprocity in UV disinfection of water. Water Sci Technol 38 (12), 145–150.
[31] Chick, H., 1908. An investigation of the laws of disinfection. J Hyg 8 (1), 92–158.
[32] Watson, H.E., 1908. A note on the variation of the rate of disinfection with change in the concentration of the disinfectant. Epidemiol Infect 8 (4), 536–542.
[33] Hijnen, W.A.M., Beerendonk, E.F., Medema, G.J., 2006. Inactivation credit of UV radiation for viruses, bacteria and protozoan (oo)cysts in water: a review. Water Res 40 (1), 3–22.
[34] Meng, X., Li, F., Yi, L., Dieketseng, M.Y., Wang, X., Zhou, L., Zheng, G., 2022. Free radicals removing extracellular polymeric substances to enhance the degradation of intracellular antibiotic resistance genes in multi-resistant *Pseudomonas Putida* by UV/$H_2O_2$ and UV/peroxydisulfate disinfection processes. J Hazard Mater 430, 128502.

[35] Song, W., Zhao, C., Zhang, D., Mu, S., Pan, X., 2016. Different resistance to UV-B radiation of extracellular polymeric substances of two cyanobacteria from contrasting habitats. Front Microbiol 7, 1208.
[36] Li, J., Hao, X., Gan, W., van Loosdrecht, M.C.M., Wu, Y., 2021. Recovery of extracellular biopolymers from conventional activated sludge: potential, characteristics and limitation. Water Res 205, 117706.
[37] Corin, N.S., Backlund, P.H., Kulovaara, M.A.M., 2000. Photolysis of the resin acid dehydroabietic acid in water. Environ Sci Technol 34 (11), 2231–2236.
[38] Kawano, A., Yamasaki, R., Sakakura, T., Takatsuji, Y., Haruyama, T., Yoshioka, Y., Ariyoshi, W., 2020. Reactive oxygen species penetrate persister cell membranes of *Escherichia coli* for effective cell killing. Front Cell Infect Microbiol 10, 496.
[39] Joyshree, M., Pandey, S., Basu, S., 2023. Enzyme assays of *E. coli* and *Bacillus sp.* treated with Fe doped MgO nanoparticles. Biol Bull 50 (4), S610–S616.
[40] Nimse, S.B., Pal, D., 2015. Free radicals, natural antioxidants, and their reaction mechanisms. RSC Adv 5 (35), 27986–28006.
[41] Surur, A.K., Momesso, V.M., Lopes, P.M., Ferrisse, T.M., Fontana, C.R., 2023. Assessment of synergism between enzyme inhibition of Cu/Zn-SOD and antimicrobial photodynamic therapy in suspension and *E. coli* biofilm. Photo Photodyn Ther 41, 103185.
[42] Kolappan, A., Satheesh, S., 2011. Efficacy of UV treatment in the management of bacterial adhesion on hard surfaces. Pol J Microbiol 60 (2), 119–123.